Journal of Inorganic Biochemistry 105 (2011) 1187–1195

Contents lists available at ScienceDirect

Journal of Inorganic Biochemistry

journal homepage: www.elsevier.com/locate/jinorgbio

Synthesis, crystal structures and spectroscopy of meclofenamic acid and its metal complexes with manganese(II), copper(II), zinc(II) and cadmium(II). Antiproliferative and superoxide dismutase activity

Dimitra Kovala-Demertzi [a,*], Malgorzata Staninska [a], Isabel Garcia-Santos [b], Alfonso Castineiras [b], Mavroudis A. Demertzis [a]

[a] Inorganic and Analytical Chemistry, Department of Chemistry, University of Ioannina, 45100 Ioannina, Greece
[b] Departamento de Quımica Inorganica, Universidad de Santiago de Compostela, E-15706 Santiago de Compostela, Spain

ARTICLE INFO

Article history:
Received 1 March 2011
Received in revised form 30 May 2011
Accepted 31 May 2011
Available online xxxx

Keywords:
Metal complexes
Meclofenamic acid
Crystal structures
Spectroscopic studies
Antineoplastic activity
Sod activity

ABSTRACT

Some new complexes of meclofenamic acid (N-(2,6-dichloro-m-tolyl)anthranilic acid), Hmeclo (**1**), with potentially interesting biological activities are described. Complexes [Mn(meclo)$_2$] (**2**), [Cu(meclo)$_2$(H$_2$O)$_2$] (**3**), [Zn(meclo)$_2$(H$_2$O)$_2$] (**4**) and [Cd(meclo)$_2$(H$_2$O)$_2$] (**5**) were prepared and structurally characterized by means of vibrational, electronic and ^{1}H and ^{13}C NMR spectroscopies. The crystal structure of complexes [Cu$_4$(meclo)$_6$(OH)$_2$(DMSO)$_2$]•2DMSO (**3a**) and [Cd(meclo)$_2$(DMSO)$_3$] (**5a**) have been determined by X-ray crystallography. Complex (**3a**) is a centrosymmetric tetramer built up around the planar cyclic Cu$_2$(OH)$_2$ unit. Complex **5a** is mononuclear seven-coordinated complex with the meclofenamato ligand behaving as a bidentate deprotonated chelating ligand. Intra and intermolecular hydrogen bonds stabilize these two structures, while the crystal packing is determined by π–π and C—H⋯π interactions. Meclofenamic acid and its metal complexes have been evaluated for antiproliferative activity *in vitro* against the cells of three human cancer cell lines, MCF-7 (breast cancer cell line), T24 (bladder cancer cell line), and A-549 (non-small cell lung carcinoma), and a mouse fibroblast L-929 cell line. Complex **5** exhibits the highest selectivity against MCF-7 and **4** shows the highest selectivity against T-24. Complexes **2**–**5** were found to be more potent cytotoxic agents against T-24 and complex **5** against MCF-7 cancer cell lines than the prevalent benchmark metallodrug, *cis-platin*. The superoxide dismutase activity was measured by the Fridovich test which showed that complex [Cu(meclo)$_2$(H$_2$O)$_2$] is a good superoxide scavenger.

1. Introduction

Meclofenamic acid (N-(2,6-dichloro-m-tolyl)anthranilic acid), HMeclo, is a non-steroidal anti-inflammatory drug (NSAID) from the family of fenamates with marked analgesic properties and is used in the treatment of osteoarthritis (OA), rheumatoid arthritis (RA) and other painful musculoskeletal diseases. Chemically, it resembles mefenamic and flufenamic acids and other fenamates in clinical use. The mode of action of the NSAIDs is attributed primarily to the inhibition of prostaglandins (PG) synthesis, and more specifically inhibition of the cyclo-oxygenase enzyme system, Cox, Cox-1 and Cox-2. Inhibition of the Cox-2 system results in anti-inflammatory action, while inhibition of the Cox-1 enzyme system results in anti-inflammatory action as well as gastric irritation [1]. However, accumulating evidence indicates that fenamates and meclofenamic acid also modulate a diversity of ion channels through a pathway that may be independent of the cyclooxygenase–prostaglandin mechanism [2]. It was found that meclofenamic acid results in the generation of potent and selective Cox-2 inhibitors [1]. New studies from the last years revealed that in addition to arthritis and pain, cancer and neurodegenerative diseases like Alzheimer's disease could potentially be treated with Cox-2 inhibitors [3,4]. Some researchers propose that NSAIDs, in addition to their inhibitory effects on the synthesis of PGs, may also inhibit the production, or act as scavengers of free radicals [5–8].

Metal complexes with active drugs as ligands are a research area of increasing interest for inorganic and medicinal chemistry and have concentrated much attention as an approach to new drug development [9,10]. The synthesis of metal complexes with NSAIDs as ligands has acquired new impetus in the past decade. The information collected from the preparative, structural and reactivity studies have high significance for several fields which span from the bio-sciences to the material sciences. The combination of two or more different species into the same compound may bring to a multi-therapeutic agent which can be expanded by the synergic action of the metal residue once the co-ordination compound dissociates inside the target tissue [12,13,15,17].

* Corresponding author. Tel.: +30 2651008425; fax: +30 2651008791.
E-mail address: dkovala@cc.uoi.gr (D. Kovala-Demertzi).

0162-0134/$ – see front matter © 20112011 Elsevier Inc. All rights reserved.
doi:10.1016/j.jinorgbio.2011.05.025

The coordination chemistry of NSAIDs has been studied by several groups worldwide. Some complexes have increased pharmaceutical or biological activity with respect to the drug or are interesting from a purely chemical point of view [10–17]. A review of the synthesis and crystal structures of a number of anti-inflammatory compounds as ligands in organotin complexes and a review of copper complexes with NSAIDs have been reported [6,10,14,16]. Crystal structures of organotin meclofenamic complexes were reported by our group. The [Ph_3Sn(Meclo)] complex exhibited high cytotoxic activity against cancer cell lines and was found to be a promising anti-mycobacterial lead compound, displaying high activity against M. tuberculosis H37Rv [17].

Copper(II)-complexes, including Cu-NSAIDs, exhibit significant anti-inflammatory activities as well as superoxide dismutase (SOD) mimetic activity. SODs, a family of metalloenzymes, catalyses the dismutation of superoxide radical anions to the non-radical products oxygen and hydrogen peroxide and protects living cells from damage induced by reactive oxygen species (ROS). The use of SOD as a pharmaceutical has been proposed for treatment of a number of diseases including, hyperoxia, reperfusion injury, acquired immune deficiency syndrome (AIDS) disease auto-immune deficiency disease (AIDS), ulcerative colitis, bronchopulmonary dysplasia in premature neonates, as well as inflammation and inflammation-associated diseases, such as rheumatoid arthritis (RA) and osteoarthritis (OA) [6]. Although there is much interest in the use of SOD for pharmaceutical purposes, its practical use in biological systems is problematic due to difficulties associated with the systematic infection of protein, i.e. the circulation lifetime, cell impermeability, immunogenicity, tissue targeting, antigenicity and high costs. To avoid such limitations, there has been considerable interest in developing synthetic SOD mimics that have low molecular weight, biological stability, and membrane permeability and are nontoxic and cost-effective [6,18,19]. However, the development of new synthetic compounds that act as mimetics of SOD and catalase has offered an alternative approach with some promise. Use of such compounds in mouse models has been effective in attenuating oxidative stress-associated disease processes and leads to extension of lifespan [20,21].

We have prepared novel complexes of meclofenamic acid, Scheme 1, with Mn(II), Cu(II), Zn(II) and Cd(II), [$Mn(meclo)_2$], [$Cu(meclo)_2(H_2O)_2$], [$Zn(meclo)_2(H_2O)_2$], and [$Cd(meclo)_2(H_2O)_2$] in order to obtain information on structure–activity relationships for systems involving metal atoms. The cytotoxic activity of meclofenamic acid and its metal complexes have been evaluated for antiproliferative activity *in vitro* against the cells of three human cancer cell lines: MCF-7 (human breast cancer cell line), T24 (bladder cancer cell line), A-549 (non-small cell lung carcinoma) and a mouse L-929 (a fibroblast-like cell line cloned from strain L). Also, the superoxide dismutase activity was measured and IC_{50} value was determined by the Fridovich test [22]. Herein, the goal is to define the probability to extend the pharmacological profile of meclofenamic acid, in order to discover new properties such as anti-cancer activity and SOD activity, to prepare new compounds, complexes of meclofenamic acid with essential metal ions, which probably would exhibit improved or different biological and pharmaceutical behaviour compared to the "parent drug", meclofenamic acid.

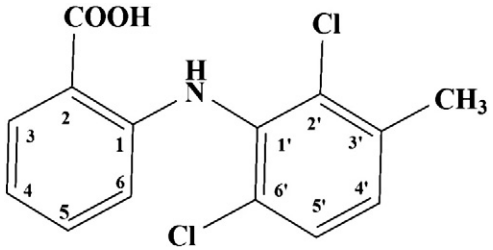

Scheme 1. The numbering scheme for Hmeclo, **1**.

2. Experimental section

2.1. General and instrumental

All reagents were commercially available (Aldrich or Merck) and used as supplied. Melting points were determined in open capillaries and are uncorrected. Infrared and far-infrared spectra were recorded on a Perkin Elmer Spectrum GX Fourier transform spectrophotometer using KBr pellets (4000–400 cm^{-1}) and nujol mulls dispersed between polyethylene disks (400–40 cm^{-1}). NMR spectra were recorded on a Bruker AV-400 spectrometer operating at 400 and 100 MHz for ^1H and ^{13}C acquisition, respectively, or on a Bruker AV-250 spectrometer operating at 250.13 and 62.90 MHz for ^1H and ^{13}C acquisition respectively. The spectra were acquired at room temperature (298 K). The splitting of proton resonances in the reported ^1H NMR spectra are defined as s = singlet, d = doublet, t = triplet, and m = multiplet. The chemical shifts are reported in ppm for ^1H and ^{13}C NMR. Samples were dissolved in $CDCl_3$ or DMSO-d^6 and spectra were obtained at room temperature with the signal of the free DMSO or $CHCl_3$ (at 2.49 and 7.24 ppm, respectively) as a reference. Elemental analyses, C, H, N and S were performed on a Carlo Erba EA (model 1108). Mass spectra were measured on an Agilent 1100 Series LC-MSD-Trap-SL spectrometer. Experimental and calcd. MS (ESI-MS) values (m/z) for each of the five compounds were identical to a significant last figure above the decimal point. Metal compositions were determined using an energy-dispersive X-ray fluorescence (EDXRF) spectroscopy arrangement.

2.2. Preparation of HMeclo and the complexes

2.2.1. Synthesis 2-[(2,6-Dichloro-3-methyl-phenyl)amino]benzoic acid (HMeclo); (**1**)

Meclofenamic was synthesized according to a published procedure from (2-carboxyphenyl)phenyliodonium and 2,6-dichloro-3-methylbenzenamine [23]. The white power was collected and recrystallized three times from ethanol to afford **1**, Yield 70%. M.p. 252–253 °C. IR (KBr): 3336 (ν(NH)); 3060br (ν(OH)); 2920, 2860 ($\nu(CH_3)$); 1656 (ν_{asym}(COO)); 1438(ν_{sym}(COO)); UV–visible (UV–vis): λ, nm (ε/logε) in DMF: 319 (3.66), 291 (3.64); in $CHCl_3$: 340 (3.53), 282 (3.49); ^1H NMR (DMSO): 13.14 s (OH); 9.15 (*s*, NH); 7.90 (*dd*, H–C(3), $J_{H(3)-H(4)} = 8.0$, $J_{H(3)-H(5)} = 1.0$); 6.77 (*t*, H–C(4), $J_{H(4)-H(5)} = 8.0$, $J_{H(4)-H(6)} = 1.1$); 7.31 (m, H–C(5)), 6.19 (*d*, H–C(6), $J_{H(6)-H(5)} = 8.4$); 7.35 (d, H4′), $J_{H(4')-H(5')} = 8.3$); 7.50 (d, H5′), $J_{H(5')-H(4')} = 8.3$); 2.38 (s, 3′ Me); ^{13}C NMR: 170.0 (COOH); 147.1 (C(1)); 111.7 (C(2)); 131.5 (C(3)); 117.3 (C(4)); 134.6 (C(5)); 112.9 (C(6)); 134.1 (C(1′)); 133.5 (C(2′)); 130.5 (C(3′)); 129.3 (C(4′)); 128.8 (C(5′)); 130.6 (C(6′)); 20.1 (3′ Me); ^1H NMR ($CDCl_3$): 9.21 (*s*, NH); 8.07 (*d*, H–C(3), $J_{H(3)-H(4)} = 6.7$); 6.79 (*t*, H–C(4), $J_{H(4)-H(5)} = 7.6$, $J_{H(4)-H(6)} = 1.1$); 7.22 (m, H–C(5)), 6.33 (*d*, H–C(6), $J_{H(6)-H(5)} = 8.4$); 7.14 (d, H4′), $J_{H(4')-H(5')} = 8.3$); 7.32 (d, H5′), $J_{H(5')-H(4')} = 8.2$); 2.41 (s, 3′ Me); ^{13}C NMR: 172.1 (COOH); 148.5 (C(1)); 110.4 (C(2)); 132.3 (C(3)); 117.4 (C(4)); 134.9 (C(5)); 113.1 (C(6)); 135.1 (C(1′)); 134.7 (C(2′)); 131.6 (C(3′)); 128.8 (C(4′)); 127.8 (C(5′)); 136.6 (C(6′)); 20.6 (3′ Me); Mass spectrum, MS (electrospray ionization, ESI, m/z): 297 $[\mathbf{1}+H]^+$, 612$[\mathbf{1_2}+H_3O]^+$. Anal. calc. for $C_{14}H_{11}Cl_2NO_2$ (296.13 g mol^{-1}): C, 56.8; H, 3.7; N, 4.7; found: C, 56.2, H, 3.9; N, 4.3%.

2.2.2. Synthesis of [Mn(meclo)$_2$]; (**2**)

Anhydrous manganese(II) acetate ([$Mn(CH_3COO)_2$]) (0.0216 g, 0.125 mM) was dissolved in methanol (2 mL) and this solution was added to a solution of meclofenamic acid (0.0740 g, 0.25 mM) in methanol (2 mL). Drops of triethylamine ($N(eth)_3$) were added to the solution till the apparent pH value was ~7. The reaction mixture was stirred for 4 h at room temperature and then it was left to the refrigerator overnight. Drops of cold distilled water were added to the solution and a whitish precipitate was collected by filtration. The powder was filtered and washed with cold MeOH/H_2O 1/1 (1:1), and

dried in vacuo to afford (**2**), yield 47%. M.p. 150–151 °C IR (cm^{-1}): 3266 m, ν(NH); 3070 m 2983 m, ν(CH3); 1615 s, ν_{asym}(COO); 1394 s, ν_{sym}(COO); 438 ms, ν(Mn-O_{H2O}); 366, 277 ms, ν(Mn-O_{oco}). UV–vis: λ, nm (ε/logε) in DMF:415sh (1.51), 364 (2.37), 321 (4.10), 294 (4.08); in $CHCl_3$: 493sh (1.63), 381 (2.46), 337 (3.84), 283 (3.85). μ_{eff} = 5.66 MB. Mass spectrum, MS (atmospheric pressure chemical ionization, APCI, m/z): 664 [**2** + H_3O]$^+$, 296 [**1** + H]$^+$. Anal. calc. for $C_{28}H_{20}Cl_4MnN_2O_4$ (645.2 g mol^{-1}): C, 52.1; H, 3.1; N, 4.3; Mn, 8.5 found: C, 52.3, H, 3.2; N, 4.2; Mn, 8.8%. The complex is soluble in DMSO, DMF, MeOH, Benzene, toluene, CH_2Cl_2, and $CHCl_3$.

*2.2.3. Synthesis of [Cu(meclo)$_2$(H_2O)$_2$]; (**3**)*

Copper(II) acetate monohydrate ([$Cu(CH_3COO)_2(H_2O)]_2$) (0.0250 g, 0.125 mM) was dissolved in methanol (2 mL) and this solution was added to a solution of meclofenamic acid (0.0740 g, 0.25 mM) in methanol (2 mL). Drops of $N(eth)_3$ were added to the solution till the apparent pH value was ~7. The reaction mixture was stirred for 4 h at room temperature and then it was left to the refrigerator overnight. The green powder was filtered and washed with cold MeOH and dried in vacuo to afford (**3**), yield 69%. D.p. 190–192 °C. IR (cm^{-1}): 3312 m, ν(NH); 3070 m 2923 m, $\nu(CH_3)$; 1618 s, ν_{asym}(COO); 1391 s, ν_{sym}(COO); 480 ms, ν(Cu-O_{H2O}); 375 m, 327 m, 245 ms, ν(Cu-O_{oco}). UV–vis: λ, nm (ε/logε) in DMF: 733 (2.25), 321 (4.13), 281 (4.16); in $CHCl_3$: 682 (1.83), 339 (4.07), 381 (4.06), 283 (3.85). μ_{eff} = 1.94 MB.Mass spectrum, MS (Electrospray Ionization, ESI, m/z): 652 [**3**-2H_3O]$^-$, 295 [**1**-H]$^-$. Anal. calc. for $C_{28}H_{24}Cl_4CuN_2O_6$ (689.8 g mol^{-1}): C, 48.9; H, 3.5; N, 4.1; Cu, 9.2 found: C, 49.1, H, 3.2; N, 4.2; Cu, 8.9%. The complex is soluble in DMSO, DMF, MeOH, EtOH, MeCN, benzene, and toluene and slightly soluble in CH_2Cl_2 and $CHCl_3$. Recrystallization of **3** from DMSO solution gives green single-crystals of the tetramer complex [$Cu_4(meclo)_6(OH)_2(DMSO)_2$]•2DMSO (**3a)** suitable for X-ray structure determination.

*2.2.4. Synthesis of [Zn(meclo)$_2$(H_2O)$_2$]; (**4**)*

Zinc(II) acetate dihydrate ([$Zn(CH_3COO)_2(H_2O)_2$]) (0.0274 g, 0.125 mM) was dissolved in methanol (2 mL) and this solution was added to a solution of meclofenamic acid (0.0740 g, 0.25 mM) in methanol (2 mL). The same procedure as in Section 2.2.2 was followed. Yellow powder (**4**), yield 29%. M.p. 140–141 °C. IR (cm^{-1}): 3295 m, ν(NH); 3068 m 2986 m, $\nu(CH_3)$; 1618 s, ν_{asym}(COO); 1397 s, ν_{sym}(COO); 467 ms, ν(Zn-O_{H2O}); 380 m, 303 m, 270 ms, ν(Zn-O_{oco}). ^{1}H NMR (DMSO): 10.23 (*s*, NH); 8.00 (*d*, H–C(3), $J_{H(3)-H(4)}$ = 9.0); 6.67 (*t*, H–C(4), $J_{H(4)-H(5)}$ = 7.4,); 7.16 (m, H–C(5)), 6.12 (*d*, H–C(6), $J_{H(6)-H(5)}$ = 8.2); 7.19 (d, H4′), $J_{H(4')-H(5')}$ = 8.3); 7.38 (d, H5′), $J_{H(5')-H(4')}$ = 8.3); 2.30 (s, 3′ Me); ^{13}C NMR: 173.6 (COOH); 146.2 (C(1)); 132.0 (C(3)); 116.7 (C(4)); 135.5 (C(5)); 112.3 (C(6)); 133.3 (C(1′)); 132.1 (C(2′)); 130.2 (C(3′)); 128.5 (C(4′)); 127.9 (C(5′)); 136.2 (C(6′)); 20.1 (3′ Me); ^{1}H NMR ($CDCl_3$): 9.42 (*s*, NH); 8.00 (*d*, H–C(3)); 6.63 (*t*, H–C(4), $J_{H(4)-H(5)}$ = 7.2); 7.17 (d, H–C(5), J(5–4) = 8.1), 6.25 (*d*, H–C(6), $J_{H(6)-H(5)}$ = 8.3); 6.97 (d, H4′), $J_{H(4')-H(5')}$ = 8.3); 7.21 (d, H5′), $J_{H(5')-H(4')}$ = 8.2); 2.28 (s, 3′ Me); ^{13}C NMR: 175.2 (COOH); 147.25 (C(1)); 113.6 (C(2)); 131.1 (C(3)); 117.1 (C(4)); 135.9 (C(5)); 115.2 (C(6)); 134.3 (C(1′)); 133.3 (C(2′)); 129.1 (C(3′)); 127.0 (C(4′)); 127.9 (C(5′)); 136.2 (C(6′)); 20.5 (3′ Me); Mass spectrum, MS (APCI, m/z): 728 [**4** + 2HO]$^-$, 295 [**1**-H]$^-$. Mass spectrum, MS (Electrospray Ionization, ESI, m/z): 753 [**4** + 2CH_3O^-]$^-$, 1345 [**4**$_2$-2H_3O]$^-$, 569 [**4**-2Cl–CH_3]$^+$. Anal. calc. for $C_{28}H_{24}Cl_4N_2O_6Zn$ (691.6 g mol^{-1}): C, 48.6; H, 3.5; N, 4.1; Zn, 9.5 found: C, 48.4, H, 3.4; N, 4.2; Zn, 9.6%. The complex is soluble in DMSO and DMF and slightly soluble in CH_2Cl_2, $CHCl_3$.

*2.2.5. Synthesis of [Cd(meclo)$_2$(H_2O)$_2$]; (**5**)*

Cadmium(II) chloride dihydrate ($CdCl_2$•2H_2O) (0.1097 g, 0.25 mM)) was dissolved in methanol (2 mL) and this solution was added to a solution of meclofenamic acid (0.0740 g, 0.25 mM) in methanol (2 mL). The same procedure as in Section 2.2.3 was followed. Yellow powder (**5**), yield 95%. M.p. 191–192 °C. IR (cm^{-1}): 3251 m, ν(NH); 3068 m 2986 m, $\nu(CH_3)$; 1618 s, ν_{asym}(COO); 1390 s, ν_{sym}(COO); 430 ms, ν(Cd-O_{H2O}); 368 m, 304 m, ν(Cd-O_{oco}). ^{1}H NMR (DMSO): 10.33 (*s*, NH); 8.02 (*dd*, H–C(3), $J_{H(3)-H(4)}$ = 7.4); 6.74 (*t*, H–C(4), $J_{H(4)-H(5)}$ = 7.4); 7.21 (t, H–C(5)), $J_{H(5)-H(45)}$ = 7.4);), 6.15 (*d*, H–C(6), $J_{H(6)-H(5)}$ = 8.1); 7.32 (d, H4′), $J_{H(4')-H(5')}$ = 8.2); 7.48 (d, H5′), $J_{H(5')-H(4')}$ = 8.2); 2.38 (s, 3′ Me); ^{13}C NMR: 173.9 (COOH); 146.1(C(1)); 131.9 (C(3)); 116.7 (C(4)); 135.5 (C(5)); 112.2 (C(6)); 133.3 (C(1′)); 132.4 (C(2′)); 130.2 (C(3′)); 128.6 (C(4′)); 128.0 (C(5′)); 136.3 (C(6′)); 20.2 (3′ Me); Mass spectrum, MS (electrospray ionization, ESI, m/z): 632 [**5**-2Cl$^-$]$^+$, 764 [**5** + Na]$^+$, 741[**5** + 2H]$^+$. Anal. calc. for $C_{28}H_{24}CdCl_4N_2O_6$ (738.67.6 g mol^{-1}): C, 45.5; H, 3.3; N, 3.8; Zn, 15.2 found: C, 45.6, H, 3.4; N, 3.9; Zn, 15.3%. The complex is soluble in DMSO and DMF and slightly soluble in CH_2Cl_2, $CHCl_3$. Recrystallization of **5** from DMSO solution gives single crystals of [Cd(meclo)$_2$(DMSO)$_3$] (**5a)** suitable for X-ray structure determination.

2.3. X-ray crystallography

A green needle crystal of [$Cu_4(meclo)_6(OH)_2(DMSO)_2$]•2DMSO (**3a**) and a colourless plate crystal of [Cd(meclo)$_2$(DMSO)$_3$] (**5a**) were mounted on a glass fiber and used for data collection. Crystal data were collected at 100(1) K, using a Bruker X8 KappaAPEXII diffractometer and a Bruker SMART CCD 1000 diffractometer for **3a** and **5a** respectively. Graphite monochromated MoK(alpha) radiation was used throughout. The data were processed with APEX2 and with SAINT for **3a** and for **5a** respectively. The data were corrected for absorption using SADABS (transmissions factors: 1.000–0.0.904) and (transmissions factors: 1.000–0.887) for **3a** and for **5a** respectively [24]. The structures were solved by direct methods using the program SHELXS-97 and refined by full-matrix least-squares techniques against F^2 using SHELXL-97 [25]. Positional and anisotropic atomic displacement parameters were refined for nonhydrogen atoms. Hydrogen atoms were located in difference maps and included as fixed contributions riding on attached atoms with isotropic thermal parameters 1.2 times those of their carrier atoms. The H atoms of methyl groups and isotropically refined atoms were included in geometrically idealized positions. Criteria of a satisfactory complete analysis were the ratios of "rms" shift to standard deviation less than 0.001 and no significant features in final difference maps. The C atoms of the methyl groups in each ligand for **3a** showed disorder and was refined using a split with 50% occupancy for each "meta" position (C24/C25, C44/C45 and C64/C65). The lowest (−1.68 e $Å^{-3}$) and highest (2.44 e $Å^{-3}$) peaks for **5a** in the final difference Fourier map are located close to the Cl23 atom at distances of 0.76 and 0.79 Å, respectively. Molecular graphics were performed from PLATON [26]. A summary of the crystal data, experimental details and refinement results is listed in Table 1.

2.4. Antiproliferative assay in vitro

Compounds: Test solutions of the compounds tested (1 mg/mL) were prepared by dissolving the substance in 100 μL of DMSO completed with 900 μL of tissue culture medium. Afterwards, the tested compounds were diluted in culture medium to reach the final concentrations of 100, 50, 10, 1 and 0.1 ng/μL. The solvent (DMSO) in the highest concentration used in test did not reveal any cytotoxic activity.

2.4.1. Cells

The cell lines are maintained in the Cell Culture Collection of the University of Ioannina. Twenty-four hours before addition of the tested agents, the cells were plated in 96-well plates at a density of 10^4 cells per well. The MCF-7 cells were cultured in the D-MEM (Modified Eagle's Medium) medium supplemented with 1% antibiotic and 10% fetal calf serum. L-929 cells were grown in Hepes-buffered RPMI 1640 medium supplemented with 10% fetal calf serum,

Table 1
Selected crystallographic data for **3a** and **5a**.

	$[Cu_4(meclo)_6(OH)_2(DMSO)_2]\cdot 2DMSO$	$[Cd(meclo)_2(DMSO)_3]$
Empirical formula	$C_{92}\ H_{80}\ Cl_{12}\ Cu_4\ N_6\ O_{18}\ S_4$	$C_{34}\ H_{38}\ Cd\ Cl_4\ N_2\ O_7\ S_3$
Formula weight	2365.42	937.04
Temperature	100(2) K	110(2) K
Wavelength	0.71073	0.71073
Crystal system, space group	Monoclinic, P 21/n	Triclinic, P −1
Unit cell dimensions		
a (Å)	8.4916(5)	8.6917(17)
b (Å)	25.2754(17)	9.2754(18)
c (Å)	23.1572(16)	24.612(5)
α (°)	90	85.617(3)
β (°)	93.224(3)	83.067(3)
γ (°)	90	73.185(3)
Volume ($Å^3$)	4962.3(6)	1883.7(6)
Z, Calculated density (Mg/m^3)	2, 1.583	2, 1.652
Absorption coef. (mm^{-1})	1.322	1.080
F(000)	2404	952
Crystal size (mm)	0.47 × 0.05 × 0.05	0.27 × 0.23 × 0.06
θ range for data collection (°)	1.19–26.02	0.83–26.37
Limiting indices	−10<=h<=10, 0<=k<=31, 0<=l<=28	−10<=h<=10, −11<=k<=11, 0<=l<=30
Reflections collected/unique	74,833/9796 [R(int) = 0.0671]	21,646/7683 [R(int) = 0.0348]
Absorption correction	Empirical	Empirical
Max. and min. transmission	0.9369 and 0.5755	0.9380 and 0.7592
Refinement method	Full-matrix least-squares on F^2	Full-matrix least-squares on F^2
Data/restraints/parameter	9796/0/640	7683/0/460
Goodness-of-fit on F^2	1.022	1.091
Final R indices [I>2sigma(I)]	$R_1 = 0.0517$, $wR_2 = 0.1061$	$R_1 = 0.0558$, $wR_2 = 0.1100$
R indices (all data)	$R_1 = 0.1033$, $wR_2 = 0.1300$	$R_1 = 0.0801$, $wR_2 = 0.1218$
Larg. diff. peak and hole ($e.Å^{-3}$)	0.876 and −0.687	2.445 and −1.684

penicillin (50 U/mL) and streptomycin (50 mg/mL). A-549 cells were grown in F-12K Ham's medium supplemented with 1% glutamine, 1% antibiotic/antimycotic, 2% $NaHCO_3$ and 10% fetal calf serum. The cell cultures were maintained at 37 °C in a humid atmosphere saturated with 5% CO_2. Cell number was counted by the Trypan blue dye exclusion method. MCF-7, L-929 and A-549 cells were determined by the sulforhodamine B assay [27], while T-24 cells by the MTT assay [28]. The *in vitro* tests were performed as described previously [29].

2.5. Superoxide dismutase assay

SOD activity of complexes **2**–**5** and the parent drug **1** was determined by using their ability to inhibit the reduction of nitro blue tetrazolium (NBT) [22,30]. The reaction system contained 0.2 mM xanthine and 0.6 mM NBT in 0.1 M phosphate buffer pH 7.8. The tested compounds were dissolved in DMF and the final concentration of DMF in the reaction mixture was 1% in 0.1 M phosphate buffer pH 7.8. The measured concentrations of the compounds were 0.5 μM, 1.0 μM, 1.5 μM, 2.0, μM, 2.5 μM, 4 μM, 5 μM, 7.5 μM and 10 μM. 0.07 U/mL, xanthine oxidase was added to the reaction to start. Each experiment was performed in triplicate.

3. Results and discussion

3.1. Synthetic aspects

Compound **1** was synthesized by the condensation of (2-carboxyphenyl)phenyliodonium, with 2,6-dichloro-3-methylbenzenamine in the presence of anhydrous copper(II) acetate as described in the literature [19]. Compounds **2**–**5** were obtained by the aerobic reaction of metal(II) acetates Mn(II), Cu(II) and Zn(II) or of Cd(II) chloride in the presence of drops of triethylamine till the apparent pH value was 7. The molar ratio for all the reactions (reactions (1–3) was 1:2 M/L.

$$[Mn(CH_3COO)_2] + Hmeclo \rightarrow [Mn(meclo)_2] + 2CH_3COOH \quad (1)$$

$$[Cu(CH_3COO)_2(H_2O)]_2 + Hmeclo \rightarrow [Cu(meclo)_2(H_2O)_2] + 2CH_3COOH \quad (2)$$

$$[Zn(CH_3COO)_2(H_2O)_2] + Hmeclo \rightarrow [Zn(meclo)_2(H_2O)_2] + 2CH_3COOH \quad (3)$$

$$CdCl_2\cdot 2H_2O + Hmeclo \rightarrow [Cd(meclo)_2(H_2O)_2] + 2HCl \quad (4)$$

Recrystallization of $[Cu(meclo)_2(H_2O)_2]$ (**3**) from DMSO solution gives the complex $[Cu_4(meclo)_6(OH)_2(DMSO)_2]\cdot 2DMSO$ (**3a**). In the presence of DMSO a transformation of the monomer (**3**) to a tetramer (**3a**) occurs. In this case hydrolysis of water and aggregation occurs in the presence of DMSO and that brings about compound **3a** according to the reaction

$$4[Cu(meclo)_2(H_2O)_2] + 4DMSO \rightarrow [Cu_4(meclo)_6(OH)_2(DMSO)_2]\cdot 2DMSO + 2Hmeclo + 6H_2O$$

Recrystallization of $[Cd(meclo)_2(H_2O)_2]$ (**5**) from DMSO solution gives the complex $[Cd(meclo)_2(DMSO)_3]$ (**5a**). The coordinated molecules of water are replaced by the coordinated molecules of DMSO.

$$[Cd(meclo)_2(H_2O)_2] + 3DMSO \rightarrow [Cd(meclo)_2(DMSO)_3] + 2H_2O$$

The complexes are microcrystalline or powder-like and stable in atmospheric conditions. All the complexes are insoluble in water, except of **5** which is slightly soluble in water. Complexes **2** and **3** are soluble in the solvents Me_2CO, $CHCl_3$, CH_2Cl_2, EtOH, DMSO, DMF, THF, benzene, hexane, pentene and toluene. Complexes **4** and **5** are soluble in DMSO, DMF and slightly soluble in THF, CH_2Cl_2 and $CHCl_3$. The elemental analyses confirm their stoichiometry. The μ_{eff} values of complexes **2** and **3**show that these are high spin. The observed values of μeff = 5.66 and μeff = 1.80 BM for complexes **2** and **3** respectively are typical for mononuclear Mn(II) and Cu(II) complexes with d^5 and d^9 configuration (S = 5/2) and (S = 1/2 respectively.

3.2. Spectroscopy

3.2.1. Infrared spectroscopy

As the carboxyl hydrogen is more acidic than the amino hydrogen the deprotonation occurs in the carboxylic group. This is confirmed by the IR spectra of the complexes, showing the characteristic bands for the secondary amino groups and for the coordinated carboxylato group. A broad absorption at 3400–3300 cm^{-1} in the spectra of the complexes was attributed to the presence of coordinated water. The absence of large systematic shifts of the ν(NH) and δ(NH) bands in the spectra of the complexes compared with those of the ligand indicates that there is no interaction between the NH group and the metal ions. The ν_{as}(COO) and ν_{sym}(COO) bands of the prepared complexes are at 1615–1618 and at 1390–1397 cm^{-1} respectively; the difference Δ [ν_{as}(COO) − ν_{sym}(COO)] between these frequencies for **2**–**5** is ~220 cm^{-1}, which is close to that found for the anisobidentate chelate carboxylato group. The medium bands at ~480–430 cm^{-1} is attributed to the ν(M-O_{H2O}) stretching mode, while the bands at 370–250 cm^{-1} to the ν(M-O_{oco}) stretching mode [7,8].

3.2.2. Electronic spectroscopy

The electronic spectra of **2** and **3** were recorded in DMF and $CHCl_3$ solution. The electronic spectra of the Mn(II) complex, **2**, can be assigned six coordinate stereochemistry [7,8]. The absorption of the organic ligand tailing into the visible region obscures the very weak d–d absorption bands of the manganese(II) complex. The broad visible band envelope of **3** will contain $dxy \rightarrow dx2-y2$ and dxz, $dyz \rightarrow dx2-y2$ at six-coordinated tetragonally distorted stereochemistry. The d–d spectra of the solvated **2** and **3** can be assigned to transitions in pseudo-octahedral structures or six-coordinated tetragonally distorted stereochemistries. The solution spectral data indicate that complexes **2** and **3** are solvated with two solvent molecules coordinating in a pseudo-octahedral arrangement. The same pattern of spectrum is shown when compounds **2** and **3** are dissolved in DMF or $CHCl_3$. It is suggested that these solvent molecules are exchanged with the axial ligands of **3** (water molecules) [10,12].

3.2.3. NMR spectra

Peak assignments were based on ^{2}D NMR data {proton–proton correlated spectroscopy (^{1}H–^{1}H COSY), proton–carbon heteronuclear single-quantum coherence (^{1}H–^{13}C HSQC) and proton–carbon heteronuclear multiple-bond correlation (^{1}H–^{13}C HMBC). The downfield chemical shift for HN in the spectra of ligand indicates that this proton is involved in hydrogen bonding. The existence of the HN resonance in the ^{1}H-NMR spectra of complexes indicates that the nitrogen atom remain protonated and the downfield chemical shift for this group indicates that this proton is involved in an intramolecular hydrogen bond between the HN group and the carbonyl oxygen of the carboxylato group. In the ^{1}H and ^{13}C NMR spectra of the Zn(II) and Cd(II) complexes **4** and **5** the hydrogen and carbon atoms of the phenyl (C1–C6) ring were shifted upon coordination, which indicated variations in the electron density of the phenyl ring. Deshielding of H(3) and C(3) is observed in complexes, which should be related to the electrophilicity of the metal centers. A σ-charge donation from the COO− donor to the metal center removes electron density from the ligand and produces this deshielding. Involvement of the carboxyl group in bonding to Zn(II) and Cd(II) is confirmed by the resonances ascribed to carboxyl carbon, which exhibit the greatest shifts upon coordination. The ^{13}C-NMR spectra of the complexes reveal major changes in the exocyclic carboxylic group, indicative of metal interaction through the carboxylic group. The latter exhibits either a

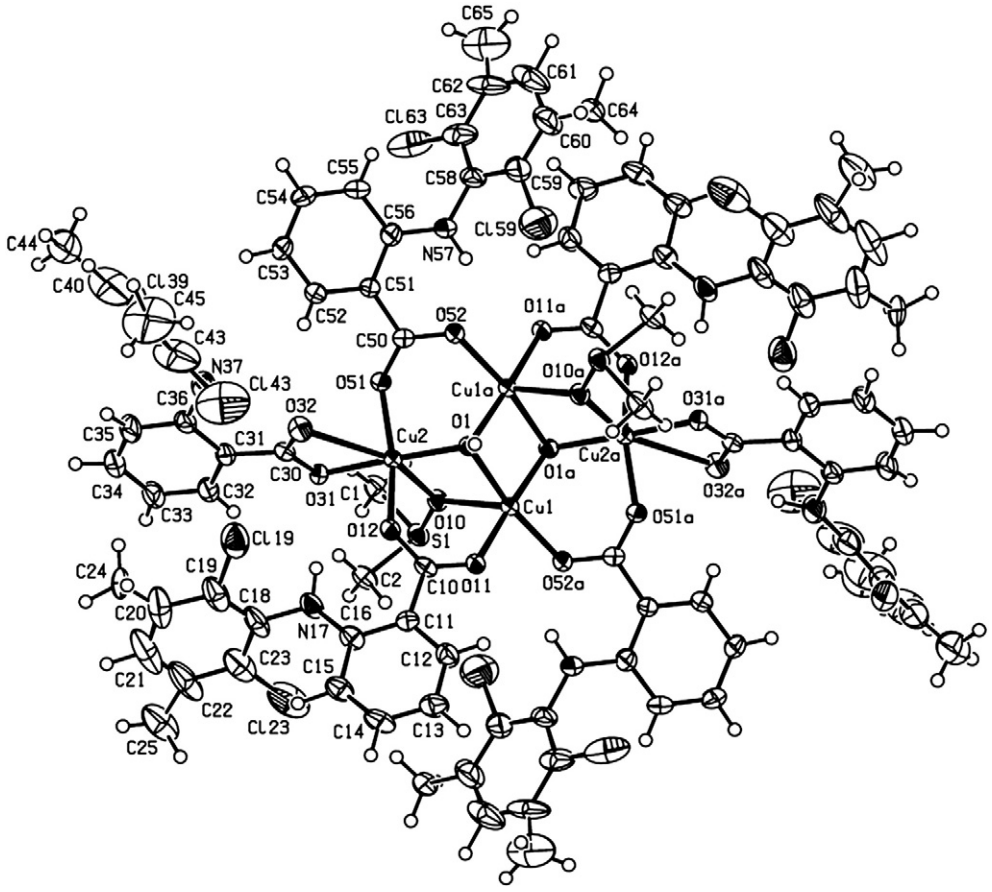

Fig. 1. Labelled ORTEP diagram of **3a**.

major downfield shift. The remaining resonances due to the aromatic carbon atoms do not shift significantly on binding to Zn(II) and Cd(II).

3.3. Crystal structures

3.3.1. Crystal structure of **3a**

A diagram of **3a** is shown in Fig. 1, and selected bond distances and angles are listed in Table 2. Compound **3a** is a centrosymmetric tetramer built up around the planar cyclic $Cu_2(OH)_2$ unit. The two oxygen atoms of this unit are linked in a μ^3-O fashion through three Cu atoms, two endo-cyclic and one exo-cyclic. The two endo and the two exo-cyclic Cu atoms are symmetrically bridged by four meclofenamato ligands through the carboxylato oxygens (Cu(1)–O(52) 1.929(3) and Cu(2)–O(51) 1.990(3) and Cu(1)–O(11) 1.934(3) and Cu(2)–O(12) 1.991(3) Å). Additional links between the endo- and exo-cyclic Cu atoms are provided by two DMSO molecules that are linked in a μ^2-O fashion and symmetrically bridge two metal centers (Cu(1)–O(10) 2.266(3) and Cu(2)–O(10) 2.277(3) Å). Each exocyclic Cu atom is also coordinated by an anisobidentate chelating meclofenamato ligand (Cu(1)–O(31) 1.936(3) Å and Cu(2)–O(32) 2.684(3) Å). The distance between the endocyclic and exocyclic Cu atoms is 3.0987(7) Å, the distance between the two endocyclic Cu centers is 2.9045(10) Å, and the distance between the two exocyclic Cu centers is 3.3276(7) Å. The coordination number is five and six for Cu(1) and Cu(2), respectively.

Table 2
Selected bond distances (A°) and angles (°) for **3a** and **5a**.

$[Cu_4(meclo)_6(OH)_2(DMSO)_2]$•2DMSO (**3a**)		$[Cd(meclo)_2(DMSO)_3]$ (**5a**)	
Cu(1)–O(52)#1	1.929(3)	Cd(1)–O(31)	2.270(3)
Cu(1)–O(11)	1.934(3)	Cd(1)–O(11)	2.352(3)
Cu(1)–O(1)#1	1.959(3)	Cd(1)–O(3)	2.376(4)
Cu(1)–O(1)	1.960(3)	Cd(1)–O(12)	2.377(4)
Cu(1)–O(10)	2.266(3)	Cd(1)–O(1)	2.389(4)
Cu(1)–Cu(1)#1	2.9045(10)	Cd(1)–O(2)	2.396(4)
Cu(1)–Cu(2)	3.0987(7)	Cd(1)–O(32)	2.418(4)
Cu(1)–Cu(2)#1	3.3278(7)		
Cu(2)–O(31)	1.936(3)		
Cu(2)–O(1)	1.944(3)		
Cu(2)–O(51)	1.990(3)		
Cu(2)–O(12)	1.991(3)		
Cu(2)–O(10)	2.277(3)		
Cu(2)–O(32)	2.684(3)		
O(1)–Cu(1)#1	1.959(3)		
O(52)#1–Cu(1)–O(11)	86.28(13)	O(31)–Cd(1)–O(11)	159.88(13)
O(52)#1–Cu(1)–O(1)#1	92.58(12)	O(31)–Cd(1)–O(3)	108.51(14)
O(11)–Cu(1)–O(1)#1	175.78(12)	O(11)–Cd(1)–O(3)	78.27(14)
O(52)#1–Cu(1)–O(1)	167.60(12)	O(31)–Cd(1)–O(12)	138.55(12)
O(11)–Cu(1)–O(1)	95.92(12)	O(11)–Cd(1)–O(12)	55.51(12)
O(1)#1–Cu(1)–O(1)	84.34(12)	O(3)–Cd(1)–O(12)	97.51(13)
O(52)#1–Cu(1)–O(10)	113.24(11)	O(31)–Cd(1)–O(1)	82.83(13)
O(11)–Cu(1)–O(10)	92.94(11)	O(11)–Cd(1)–O(1)	84.71(13)
O(1)#1–Cu(1)–O(10)	91.24(11)	O(3)–Cd(1)–O(1)	156.67(15)
O(1)–Cu(1)–O(10)	78.90(11)	O(12)–Cd(1)–O(1)	85.62(13)
O(31)–Cu(2)–O(1)	176.11(12)	O(31)–Cd(1)–O(2)	79.63(14)
O(31)–Cu(2)–O(51)	87.74(12)	O(11)–Cd(1)–O(2)	120.45(14)
O(1)–Cu(2)–O(51)	93.18(12)	O(3)–Cd(1)–O(2)	74.59(17)
O(31)–Cu(2)–O(12)	87.79(12)	O(12)–Cd(1)–O(2)	76.87(13)
O(1)–Cu(2)–O(12)	92.38(12)	O(1)–Cd(1)–O(2)	128.35(15)
O(51)–Cu(2)–O(12)	163.07(12)	O(31)–Cd(1)–O(32)	55.76(12)
O(31)–Cu(2)–O(10)	97.18(11)	O(11)–Cd(1)–O(32)	108.53(12)
O(1)–Cu(2)–O(10)	78.94(11)	O(3)–Cd(1)–O(32)	80.94(14)
O(51)–Cu(2)–O(10)	106.36(11)	O(12)–Cd(1)–O(32)	163.67(12)
O(12)–Cu(2)–O(10)	90.40(11)	O(1)–Cd(1)–O(32)	89.60(13)
O(31)–Cu(2)–O(32)	54.43(11)	O(2)–Cd(1)–O(32)	117.86(13)
O(1)–Cu(2)–O(32)	129.45(11)		
O(51)–Cu(2)–O(32)	75.50(11)		
O(12)–Cu(2)–O(32)	88.64(11)		
O(10)–Cu(2)–O(32)	151.61(10)		
Cu(2)–O(1)–Cu(1)#1	117.00(14)		
Cu(2)–O(1)–Cu(1)	105.08(12)		
Cu(1)#1-O(1)–Cu(1)	95.66(12)		
Cu(1)–O(10)–Cu(2)	86.02(10)		

Analysis of the shape determining angles for Cu(1), using the approach of Reedijk and coworkers [31], yields τ $((\alpha-\beta)/60)$ a value of 0.14 for Cu(1) (τ = 0.0 and 1.0 for square–pyramidal (SP) and trigonal–bipyramidal (TBP) geometries respectively). The metal coordination geometry is therefore described as distorted square pyramidal for Cu(1) with the O(10) atom occupying the apical position for Cu(1). The donor O(10) is chosen as apex by the simple criterion that it should not be one of the oxygens which define either of the two largest L–Cu–L angles, α and β [29]. The metal coordination geometry is described as distorted octahedral for Cu(2). The phenyl rings are planar. The dihedral angles between the planes of the phenyl rings are 66.6(3) and 61.1(6)° for the bidentate bridging the Cu(1)–Cu(2) and Cu(2)–Cu(1a) metal centers respectively. The dihedral angle for the anisobidentate chelating ligand is 53.3(3)°, while in meclofenamic acid, the two planes are virtually perpendicular, the corresponding angle being 81° [32]. The amino-benzoate portion of each carboxylato ligand is effectively planar which facilitates the formation of intramolecular N(17)–H…O(12), N(37)–H…O(32) and N(57)–H…O(52) interactions of 2.669(5), 2.606(5) and 2.698(5) Å, respectively. The bidentate bridging meclofenamato has a difference of 0.011 and 0.028 Å (O(11)–C(10) 1.272(5), O(12)–C(10) 1.261(5); O(51)–C(50) 1.252(5), O(52)–C(50) 1.280(5) Å) between its C–O bonds while for the anisobidentate chelated meclofenamato this difference is 0.045 Å (O(31)–C(30) 1.289(5) O(32)–C(30) 1.244(5) Å); the variations in the C–O bond distances suggest charge delocalization over the carboxylato group COO. The different modes of bonding of the acetates, i.e. bridging or chelating, are thus easily differentiated by the relevant bond lengths. Intra and intermolecular hydrogen bonds, π–π and C—H—π interactions stabilize this structure, Table 3.

3.3.2. Crystal structure of **5a**

A diagram of **5a** is shown in Fig. 2. The complex is mononuclear with the meclofenamato ligand behaving as a bidentate deprotonated chelating ligand [Cd–O(11) 2.352(3), Cd–O(12) 2.377(4) and Cd–O(31) 2.270(3), and Cd–O(32) 2.418(4) respectively for the two ligands], coordinated to cadmium atom *via* a carboxylate oxygen atoms. The three DMSO molecules are coordinated to cadmium atom *via* the oxygen atom [Cd–O(1) 2.389(4), Cd–O(2) 2.396(4) and Cd–O(3) 2.376(4) for the three molecules of DMSO], thus rendering cadmium atom seven-coordinated. All the Cd–O distances are of the same magnitude with Cd–O(11) = 2.353(3) being the shortest and the Cd–O(32) 2.418(4) being the longest from the two carboxylato groups. The dihedral angles between the planes of the phenyl rings for **3a** are 71.3(3)° and 65.4(3)° for the two bidentate chelating ligands, respectively, while in meclofenamic acid, the two planes are virtually perpendicular, the corresponding angle being 81° [32]. The polar imino hydrogen atoms on N, participates in an intramolecular hydrogen bond. Intra and intermolecular hydrogen bonds stabilize the structure, while the crystal packing is determined by π–π and C—H—π interactions. Strong π–π interaction occur between the phenyl rings C(18)–C(32) (symmetry operation; −x, 1 − y, −z) at a centre-to-centre separation of 3.767(4) and between the phenyl rings C(38)–C(43) (symmetry operation; −x, 1 − y, 1 − z) at a centre-to-centre separation of 3.808(3), Table 3.

3.4. Pharmacology

3.4.1. Antiproliferative activity in vitro

The results of cytotoxic activity *in vitro* are expressed as IC_{50}— the concentration of compound (in μM) that inhibits a proliferation rate of the tumor cells by 50% as compared to control untreated cells, Table 4. Meclofenamic acid and the metal complexes **1**–**5** were tested for their antiproliferative activity *in vitro* against the cells of three human cancer cell lines: MCF-7 (human breast cancer cell line), T24 (bladder cancer cell line), A-549 (non-small cell lung carcinoma) and a mouse fibroblast L-929 cell line and the results are compared with the known

Table 3
C—H—–π, π–π, inter- and intra- molecular hydrogen bonds for **3a** and **5a**; Cg(1) and Cg(2) refer to the centroids C(11)–C(12)–C(13)–C(14)–C(15)–C(16) and C(58)–C(59)–C(60)–C(61)–C(62)–C(63) and Cg(3) refer to the centroid C(31)–C(32)–C(33)–C(34)–C(35)–C(36) for **3a**. Cg(1), Cg(2) and Cg(3) refer to the centroids C(18)–C(19)–C(20)–C(21)–C(22)–C(23), C(38)–C(39)–C(40)–C(41)–C(42)–C(43) and C(31)–C(32)–C(33)–C(34)–C(35)–C(36) resp., for **5a**. D and A refers to donor and acceptor respectively.

$[Cu_4(meclo)_6(OH)_2(DMSO)_2]$•2DMSO (**3a**)					
		Cg–Cg[b]	β[c]	CgI-Perp[d]	CgJ-Perp[e]
Cg(1)–>Cg(2)[vii]		4.376(3)	39.42	4.225(2)	3.381(3)
Cg(1)–>Cg(2)[vii]		4.376(3)	15.09	3.380(3)	4.225(2)
			H—Cg	C—Cg	C–H—Cg
C(3)–H(3B)–>Cg(3)[viii]			2.79	3.539(7)	120
D	H	A[b]	D ··· A	H ··· A	D - H ··· A
N(17)	H(17A)	O(12)	2.669(5)	2.05	123
N(37)	H(37A)	O(32)	2.606(5)	1.80	143
O(1)[x]	H(1)	O(20)	2.639(4) 3.190(7)	1.90	177
C(3)[ix]	H(3C)	O(32)		2.54	127
$[Cd(meclo)_2(DMSO)_3]$ (**5a**)					
		Cg–Cg[b]	β[c]	CgI-Perp[d]	CgJ-Perp[e]
Cg(1)>Cg(1)[ii]		3.767(4)	21.82	−3.497(3)	−3.497(3)
Cg(2)–>Cg(2)[iv]		3.808(3)	22.90	−3.497(3)	−3.508(2)
			H—Cg	C—Cg	C–H—Cg
C(4)–H(4B)–>Cg(3)[v]			2.63	3.476(7)	138
C(14)–H(14)–>Cg(1)[vi]			2.82	3.655(7	142
D	H	A[b]	D ··· A	H ··· A	D–H ··· A
N(17)	H(17A)	O(11)	2.630(5)	1.91	147
N(37)	H(37A)	O(31)	2.630(5)	2.03	147
C(1)[i]	H(1B)	O(2)	3.478(8)	2.56	156
C(24)[ii]	H(24C)	O(32)	3.440(9)	2.47	170
C(33)[iii]	H(33)	O(12)	3.470(8)	2.60	154
C(41)[iv]	H(41)	O(1)	3.404(6)	2.46	163

[a]Symmetry transformations, i, = −1 + x, y, z; ii, −x, 1 − y, −z; iii, 1 + x, −1 + y, z; iv, −x, 1 − y, 1 − z; v, −x, 1 + y, z; vi, −1 − x, 2 − y, −z; vii, 2 − x, 1 − y, 1 − z; viii, ½ + x, ½ − y, −1/2 + z; ix, −1/2 + x, 1/2 − y, −1/2 + z; x, 1/2 + x, 1/2 − y,1/2 + z; [b]Cg–Cg is the distance between ring centroids; [c]Where β is the angle Cg(I)–->Cg(J); [d]CgI-Perp is the perpendicular distance of Cg(I) on ring J; [e]CgJ-Perp is the perpendicular distance of Cg(J) on ring I.

chemotherapeutic *cis-platin* and related complexes of tolfenamic acid and mefenamic acid [7,8]. Meclofenamic acid exhibits poor cytotoxic activity against MCF-7 and T24 cell lines and very poor cytotoxic activity against L-929 and A-549 cell lines. Metal salts are inactive against L-929, A-549 and MCF-7 and exhibit very poor activity against T-24 cancer cell lines. Also, complex **4** is inactive against A-549 cancer cell line.

The IC_{50} values for complexes **2**–**5** range from 23–62 μM against L-929 and A-549 cancer cell lines tested. The IC_{50} values for complexes **2**–**5** range from 5 to 40 μM against MCF-7 and 3–5 μM against T-24 cancer cell while for *cis-platin* the IC_{50} values range from 1 to 42 μM against all cancer cell lines tested. Complexes **2**–**5** are less cytotoxic than *cis-platin* against L-929 ans A-549 cancer cell lines. Complexes **2**–**4** are in the same range as *cis-platin*, 4–5 times less cytotoxic than *cis-platin* while complex **5** is 1.6 times more cytotoxic than *cis-platin*. Complexes **2**–**5** are 8–13 times more cytotoxic than *cis-platin* against T-24 cancer cell lines. Selectivity was observed for complexes **4** and **5** against T-24 and for complex **5** against MCF-7

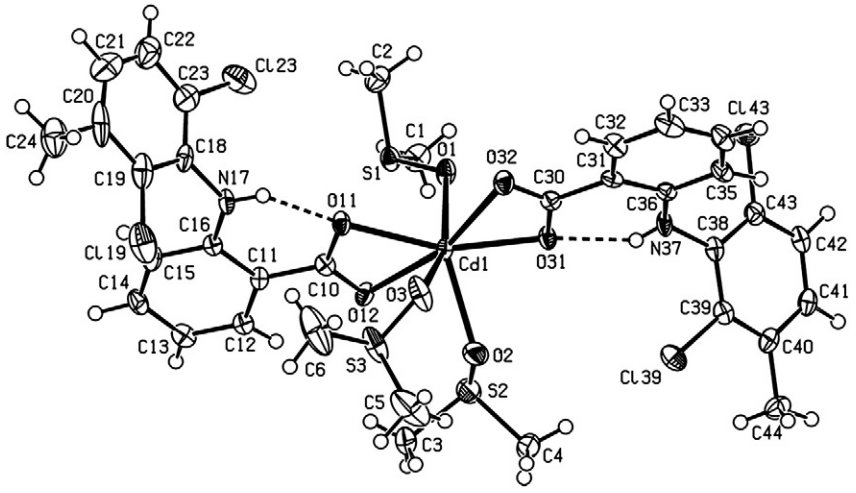

Fig. 2. Labelled ORTEP diagram of **5a**.

Table 4
The antiproliferative activity *in vitro* of **1**–**5**, related NSAIDs and metal complexes (expressed as IC_{50} (μM) against MCF-7, T-24, A-549 and L-929 cancer cell lines).

	MCF-7	T-24	A-549	L-929
HMeclo (**1**)	63.1 ± 0.4	70.2 ± 0.3	139.1 ± 0.7	133.0 ± 0.8
[Mn(meclo)$_2$] (**2**)	39.8 ± 2.4	**3.8 ± 1.3**	27.4 ± 3.2	25.3 ± 2.4
[Cu(meclo)$_2$(H$_2$O)$_2$] (**3**)	38.2 ± 0.9	**5.3 ± 0.6**	41.2 ± 5.6	61.9 ± 3.9
[Zn(meclo)$_2$(H$_2$O)$_2$](**4**)	32.5 ± 2.1	**3.2 ± 1.0**	>244 [d]	24.2 ± 2.8
[Cd(meclo)$_2$(H$_2$O)$_2$](**5**)	**5.1 ± 1.2**	**3.3 ± 1.6**	29.8 ± 1.4	22.7 ± 2.2
HTolf[a]	87.9 ± 6.3	62.4 ± 5.1	145 ± 12	214 ± 18
[Mn(tolf)$_2$(H$_2$O)$_2$][a]	41.6 ± 2.9	**3.9 ± 0.3**	65.3 ± 6.1	149 ± 6
[Cu(tolf)$_2$(H$_2$O)]$_2$[a]	26.1 ± 2.1	13. 9 ± 1.1	31.4 ± 2.2	5.3 ± 0.5
[Zn(tolf)$_2$(H$_2$O)][a]	41.3 ± 3.5	41.0 ± 2.5	57.9 ± 4.2	123 ± 6
Hmef[b]	149.2 ± 3.2	81.2 ± 4.5	168.3 ± 2.3	178.2 ± 2.8
[Mn(mef)$_2$(H$_2$O)$_2$][b]	72.6 ± 3.5	35.1 ± 1.0	>175.6[d]	>175.6 [d]
[Cu(mef)$_2$(H$_2$O)]$_2$[b]	25.1 ± 3.3	7.77 ± *2.2*	>100.3 [d]	19.5 ± 3.0
[Zn(mef)$_2$][b]	40.7 ± 5.0	37.7 ± 2.0	111.2 ± 3.0	74.4 ± 1.0
Mn(Ac)$_2$	n.o.[c]	53.4 ± 9.6	n.o.	n.o.
Cu(Ac)$_2$ H$_2$O	n.o.	50.1 ± 10.0	n.o.	233.7 ± 15.3
Zn(Ac)$_2$ 2H$_2$O	n.o.	95.7 ± 16.2	n.o.	n.o.
CdCl$_2$ 2H$_2$O	n.o.	130.7 ± 7.0	n.o.	n.o.
Cis-platin	8.0 ± 0.8	41.7 ± 4.5	1.5 ± 0.1	0.7 ± 0.1

[a] Data taken from ref. [7].
[b] Data taken from ref. [8].
[c] Activity not observed.
[d] The IC_{50} value is not possible to be calculated, since the inhibition for the higher concentration (100 μg/mL) was found to be 30–35%. In that case, the IC_{50} value will be higher than the concentration of 244 μM for the complex [Zn(meclo)$_2$(H$_2$O)$_2$](4) or higher than the concentration of 175.6 μM for the complex [Mn(mef)$_2$(H$_2$O)$_2$].

cancer cell lines. Also, it was found that the metal complexes of tolfenamic acid (Htolf), [Mn(tolf)$_2$(H$_2$O)$_2$] and [Cu(tolf)$_2$(H$_2$O)]$_2$ have shown selectivity against T-24 cell line [7,8]. Compounds **2**–**5** exhibited high activity as anticancer agents against T-24 cancer cell lines, and exhibited selectivity against the same cancer cell line. Compound **5** exhibits the highest selectivity against MCF-7 and **4** shows the highest selectivity against T-24. From the *in vitro* experimental results, it is indicated that meclofenamic acid and the metal acetates are non active or less active than their corresponding metal complexes of meclofenamic, which indicates that the mechanism of action is different.

The reported therapeutic action of these metal complexes could be either due to a small proportion of metal complexes that can bind intact to biomolecules and can be transported to the site of action, or to a ternary Metal-meclofenamic-biomolecule complex which is also the transporting agent [7]. Interestingly enough, **2**–**5** were found to be more potent cytotoxic agents against T-24 and **5** the most potent agents against MCF-7 cancer cell lines than the prevalent benchmark metallodrug, *cis-platin*, under the same experimental conditions measured by us and this assumes significance in light of the fact that *cis-platin* is undisputedly the most studied and widely used metallopharmaceutical for cancer therapy known to date.

3.4.2. Superoxide dismutase

The SOD activity was examined indirectly using the nitro blue tetrazolium assay. The SOD activity was measured by monitoring the reduction of NBT by O_2^- generated by the xanthine/xanthine oxidase system. As the reaction proceeds, the farmazan colour is developed and a colour change from yellow to blue/mauve is appeared, which is associated with an increase in the absorption spectrum at 560 nm. When a chemical inhibitor is added, the reduction reaction proceeds slowly or is totally inhibited in which instance the solution remains yellow and the rate of increase was reduced with increasing concentration. The rate of absorption change is determined and the concentration required to produce 50% inhibition (IC_{50}) be obtained by graphing the rate of NBT reduction versus the concentration or the log of the concentration of the test solution. Many low-molecular metal complexes, mainly copper, manganese complexes, have been synthesized and their SOD-like activity examined *in vitro* and *in vivo*. The IC_{50} results for a number of Cu(II)-NSAIDs using NBT assay were investigated [6,18]. Complexes exhibited SOD activity with IC_{50} values ranging from 1 to 28 μM. Very low values for a manganese superoxide dismutase mimic were reported by Nagano and coworkers (0.75 μM) and Rajan (0.75 μM) [33,34]. In both of these complexes manganese is in the divalent form. However, in dismutases containing manganese the metal is normally in the trivalent state, but can be reduced to the divalent state without any loss of enzymic activity. It is also worth noting that many of the high activity complexes are neutral rather than anionic. Complexes **2** and **3**show an IC_{50} value of 6.48 ± 0.81 and 1.78 ± 0.16 (μM) respectively, while the parent drug meclofenamic and the complexes of Zn(II) and Cd (II) did not show any SOD activity. These values indicate that **3** is a potent superoxide dismutase mimic. Similar results have been obtained for copper(II) complexes [6,18]. It was found that the IC_{50} values for the corresponding copper(II) complexes of tolfenamic and diclofenac [Cu (tolf)2(H2O)]2 and [Cu(dicl)$_2$(H$_2$O)]$_2$•2H$_2$O are 1.97 ± 0.17 and 2.13 ± 0.11(μM) respectively [16]. Among the copper(II) fenamates [18] complex **3** exhibits the highest SOD activity. Following the usual criteria advanced by Roberts and Robinson [35] the present copper(II) complex is considered as potent SOD mimic.

Acknowledgments

G.S. thanks IKY for a scholarship for her Ph.D. We thank Dr. P. Stathopoulos for low resolution mass spectra obtained on a machine funded by the Network of Research Supporting Laboratories of the University of Ioannina. We thank the NMR service of the University of Ioannina, Greece.

Appendix A. Supplementary data

Crystallographic data for the structural analysis has been deposited with the Cambridge Crystallographic Data Centre, CCDC 814419 and 814420 for compounds **3a** and **5a** respectively. Copies of this information may be obtained free of charge from The Director, CCDC, 12, Union Road, Cambridge CB2 1EZ [Fax: +44 1223 336 033] or e-mail deposit@ccdc.cam.ac.uk or http://www.ccdc.cam.ac.uk. Supplementary data associated with this article can be found, in the online version, at doi:10.1016/j.bbapap.2011.06.003.

References

[1] A.S. Kalgutkar, B.C. Crews, S.W. Rowlinson, A.B. Marnett, K.R. Kozak, R.P. Remmel, L.J. Marnett, Proc. Natl. Acad. Sci. U. S. A. 97 (2000) 925–930.
[2] O.K.-Y. Wu, Biochem. Pharmacol. 55 (1998) 543–547.
[3] Y.T. Lee, Q. Wang, Eur. J. Pharmacol. 378 (1999) 349–356.
[4] T. Kawamori, C.V. Rao, K. Seibert, B.S. Reddy, Cancer Res. 58 (1998) 409–412.
[5] H.M. Tucker, R.E. Rydel, S. Wright, S. Estus, J. Neurochem. 71 (1998) 506–516.
[6] J.E. Weder, C.T. Dillon, T.W. Hambley, B.J. Kennedy, P.A. Lay, J.R. Biffin, H.L. Regtop, N.M. Davies, Coord. Chem. Rev. 232 (2002) 95–126.
[7] D. Kovala-Demertzi, Hadjipavlou-Litina, A. Primikiri, M. Staninska, C. Kotoglou, M. A. Demertzis, Chem. Biodivers. 6 (2009) 948–960.
[8] D. Kovala-Demertzi, D. Hadjipavlou-Litina, M. Staninska, A. Primikiri, C. Kotoglou, M.A. Demertzis, J. Enzyme Inhib. Med. Chem. JEIMC 24/3 (2009) 742–752.
[9] R. Cini, Comments Inorg. Chem. 22 (2000) 151–186 [and references therein].
[10] D. Kovala-Demertzi, J. Inorg. Biochem. 79/1-4 (2000) 153–157.
[11] R. Cini, G. Tamasi, S. Defazio, M.B. Hursthouse, J. Inorg. Biochem. 101 (2007) 1140–1152.
[12] A. Theodorou, M.A. Demertzis, D. Kovala- Demertzi, E.E. Lioliou, A.A. Pantazaki, D. A. Kyriakidis, Biometals 12 (1999) 167–172.
[13] V. Dokorou, A. Primikiri, D. Kovala-Demertzi, J. Inorg. Biochem. 105 (2011) 195–201.
[14] D. Kovala-Demertzi, J. Organomet. Chem. 691 (2006) 1767–1774.
[15] E. Dubler, Met. Ions Biol. Syst. 32 (1996) 301–338.
[16] G. Tamasi, Open Crystallogr. J. 3 (2010) 41–53.
[17] D. Kovala-Demertzi, V. Dokorou, A. Primikiri, R. Vargas, C. Silvestru, U. Russo, M.A. Demertzis, J. Inorg. Biochem. 103 (2009) 738–744.
[18] D. Kovala-Demertzi, A. Galani, M.A. Demertzis, S. Skoulika, C. Kotoglou, J. Inorg. Biochem. 98 (2004) 358–364.
[19] M.N. Patel, D.S. Gandhi, P.A. Parmar, Inorg. Chem. Comm. 13 (2010) 618–621.
[20] T. Finkel, N.J. Holbrook, Nature 408 (2000) 239–247.
[21] S. Melov, J. Ravenscroft, S. Malik, M.S. Gill, D.W. Walker, P.E. Clayton, D.C. Wallace, B. Malfroy, Susan R. Doctrow, G.J. Lithgow, Science 289 (2000) 1567–1569.

[22] C. Beauchamp, I. Fridovich, Anal. Biochem. 44 (1971) 276–287.
[23] J.S. Kaltenbrom, R.A. Scherrer, F.W. Short, H.R. Beatty, M.M. Saka, C.W. Winder, J. Wax, W.R.N. Williamson, Arzneim.-Forsch. (Drug Res.) 33/1 (1) (1983) 621–627.
[24] G.M. Sheldrick, SADABS. Program for Empirical Absorptio, Correction of Area Detector Data, University of Goettingen, Germany, 1997.
[25] G.M. Sheldrick, Acta Crystallogr. A64 (2008) 112–122.
[26] A.L. Spek, PLATON. A Multipurpose Crystallographic Tool, Utrecht University, Utrecht, The Netherlands, 2003.
[27] P. Skehan, R. Storeng, D. Scudiero, A. Monks, J. Mcmahon, D. Vistica, J.T. Warren, H. Bokesch, S. Kenney, M.R. Boyol, J. Natl. Cancer Inst. 82 (1990) 1107–1110.
[28] M. Ohno, T. Abe, J. Immunol. Methods 145 (1–2) (1991) 199–203.
[29] D. Kovala-Demertzi, P.N. Yadav, J. Wiecek, S. Skoulika, T. Varadinova, M.A. Demertzis, J. Inorg. Biochem. 100 (2006) 1558–1567.
[30] J. Robak, R.J. Gryglewski, Biochem. Pharmacol. 37 (1988) 837–841.
[31] A. Addison, R.T. Nageswara, J. Reedijk, J. Van Rijn, G.C. Verschoor, J. Chem. Soc., Dalton Trans. (1984) 1349–1356.
[32] H.M.K. Murthy, M. Vijayan, Acta Crystallogr., Sect. B: Struct. Sci. 37 (1981) 1102–1105.
[33] R. Rajan, R. Rajaram, B.U. Nair, T. Ramaswami, S.K. Mandal, J. Chem. Soc., Dalton Trans. (1996) 2019–2030.
[34] K.N. Osawa, M.N. Tamura, Y. Moro-oka, T. Hirano, M. Hirobe, T. Nagano, Inorg. Chem. 32 (1993) 1879–1880.
[35] N.A. Roberts, P.A. Robinson, Br. J. Rheumatol. 24 (1985) 128–136.